

Towards a Series Elastic Actuator with Electrically Modulated Stiffness for Powered Ankle-Foot Orthoses

Edgar Bolivar*¹, David Allen*¹, Gregory Ellson², Jorge Cossio³, Walter Voit^{1,2}, and Robert Gregg^{1,3}

Abstract—Series elastic actuators offer several benefits for powered ankle foot orthoses. One major benefit they offer for this application is the reduction of motor power requirements, which enables the reduction of motor weight. However, series elastic actuators commonly have a fixed stiffness value, which only yields optimal power reduction for one set of gait parameters such as gait type, user weight, and gait speed. These parameters vary during the normal use of orthotic devices. This paper presents a new variable stiffness series elastic actuator that can compensate for these variations. Our actuator uses a dielectric elastomer as the series elastic element so that the stiffness of the actuator can be electrically modulated, unlike current variable stiffness actuators that modulate their stiffness with a second motor. Experimental results indicate the viability of this approach for modulating stiffness and verify that the actuator generates forces meaningful for gait assistance.

I. INTRODUCTION

Powered Ankle-Foot Orthoses (PAFOs) provide walking assistance to people with neuromuscular impairments [1]. Because these robotic devices integrate closely with humans in the fundamental task of locomotion, they should be both portable and compliant. This paper discusses the design and performance of a novel PAFO actuator that combines dielectric elastomer and electric motor technology to increase portability and compliance with the user.

Series Elastic Actuators (SEA), consisting of a conventional actuator connected in series through an elastic element to a load, offer several benefits for PAFOs. First, they offer a safer human-machine interface than rigid PAFO actuators do because the actuated joint is back-driveable and capable of shock absorption. Second, expensive load cells are not necessary to measure an SEA's output force. An SEA's output force can be calculated from measurement of the contraction or extension of its elastic element, reducing the cost for closed-loop force control [2]. Finally, SEA can weigh less than rigid PAFO actuators with the same peak power output capability [3]. Since walking is a cyclic process, an SEA's elastic element can absorb energy in one part of the cycle

and then release it later, reducing the peak power required from the SEA motor. Because of this power reduction, a PAFO SEA can use a smaller, lighter motor than a rigid PAFO actuator requires resulting in overall weight savings [3].

The optimal stiffness value for a PAFO SEA's elastic element (resulting in minimal actuator weight) depends on the task the PAFO user is performing (e.g. running, slow/fast walking, or stair climbing/descent) as well as the user's weight and personal gait pattern. These parameters can change during normal operation of a PAFO, so a fixed stiffness elastic element cannot always provide optimal peak power reduction. An SEA with a poorly chosen stiffness may have higher motor peak power requirements than a rigid actuator and thus demand a heavier motor than necessary [3]. Therefore, a PAFO would benefit from using a Variable Stiffness Actuator (VSA). For the purposes of this work, we use the term VSA to refer to as an SEA that can change the stiffness of its elastic element. Such a device can modulate its stiffness to compensate for changes in gait parameters.

Rigid actuators with active impedance control can imitate the compliance of VSA [2], but a disadvantage of this approach is that no energy can be stored in the actuation system without proper power electronics. In addition, limitations on the bandwidth of the controller and actuator reduces such a system's shock absorption capability [4]. VSA that use inherently compliant elements such as springs do not suffer from either of these limitations, hence this class of VSA is considered in this paper.

Grioli et al. [5] published datasheets for different VSA that describe the state of the art and reveal common trends in VSA design. VSA commonly use two electric motors: one to control their equilibrium position and another (usually smaller) to modulate their stiffness as seen in the designs of [6]–[9]. Because their stiffness regulation motors are low power, these devices usually change stiffness slowly and may not be able to change stiffness during operation [10]. In addition, these designs tend to be bulky and heavy due to their mechanical complexity. These limitations and the possibility to enhance performance motivate our design.

In our design, Dielectric Elastomers (DE) replace the elastic elements of traditional VSA. DE are flexible polymers coated with flexible electrodes that expand when energized with electrical charges. The electrical energy that actuates the DE also changes their stiffness [11]. Our approach has the following advantages over traditional VSA designs: 1) the VSA may weigh less since it does not require a motor for stiffness modulation; 2) the VSA can change stiffness

*Both authors contributed equally to this manuscript.

¹Department of Mechanical Engineering, ²Department of Materials Science & Engineering, ³Department of Bioengineering, University of Texas at Dallas, Richardson, TX 75080. {edgarbolivar, david.allen, gregory.ellson, jxc117930, walter.voit, rgregg}@utdallas.edu

This work was supported by the National Institute of Child Health & Human Development of the NIH under Award Number DP2HD080349. The content is solely the responsibility of the authors and does not necessarily represent the official views of the NIH. R. D. Gregg holds a Career Award at the Scientific Interface from the Burroughs Welcome Fund. This work was also supported by the Margaret and Eugene McDermott Graduate Fellows Program and the Defense Advanced Research Projects Agency (DARPA)/MTO Young Faculty Award (YFA) Grant No. D13AP00049.

rapidly enabling modulation of its stiffness during operation; 3) the DE could regenerate energy during operation; 4) DE can work as strain and force sensors; and 5) the PAFO can be more comfortable to wear since DE can be formed into shapes that conform to the user's body.

DE have been used as variable stiffness devices before. However, we are not aware of DE being used with an electric motor as an SEA. The designs presented in [12] and [13] both use DE as variable stiffness devices, but in these devices, the DE are also the only source of actuation. Further, in these approaches, the force output of the DE was actively modulated to produce a desired force-displacement response, much like traditional impedance control. The VSDEA presented in [14] uses DE along with a low-melting-point alloy (LMPA) device. In this approach, the stiffness is controlled by the LMPA device, and the DE serves as an actuator. In our approach, an electric motor serves as an actuator, and DE provide variable stiffness. The mechanical and electrical configuration of the DE prevents them from providing actuation. We control the actuator's stiffness by applying a voltage to the DE, and then letting the inherent material behavior provide the device's stiffness characteristics. This novel approach exploits the strengths of both the new and traditional methods of actuation.

The next section of this paper explains additional details about human gait, SEA, and DE, which are key background theory for this paper. Sec. III discusses design requirements and choices for our actuator design and then presents the novel actuator. Sec. IV presents preliminary experiments to test the device's performance and discusses future directions for the project.

II. BACKGROUND THEORY

This section will describe the motivating theory behind our design. To contextualize ankle-foot orthosis design, Sec. II-A explains the actions of the human ankle during walking. Sec. II-B explains how an SEA can reduce the motor power requirements for a PAFO and thus reduce its weight. Finally, Sec. II-C explains how DE work and how they can change stiffness.

A. Human Ankle Motion During Level-Ground Walking

PAFOs aid human locomotion by providing assistive torques to the ankle joint. Since the human ankle-foot complex can be thought of as an actuator, an understanding of its functions during walking provides valuable context for the understanding of PAFO actuator design.

A normal gait cycle is composed of two phases: stance and swing. At the beginning of the stance phase, which starts when the heel first touches the ground, the ankle-foot complex acts as a brake and shock absorption unit by resisting ankle plantarflexion [15]. Impairment of the ankle's dorsiflexion muscles, which perform this task, will create a foot slap. Once the foot is parallel to the ground, the ankle provides a stiff connection to the upper part of the body, stabilizing it during this period of locomotion. Subsequently, near the end of the stance phase, the plantarflexion muscles inject about

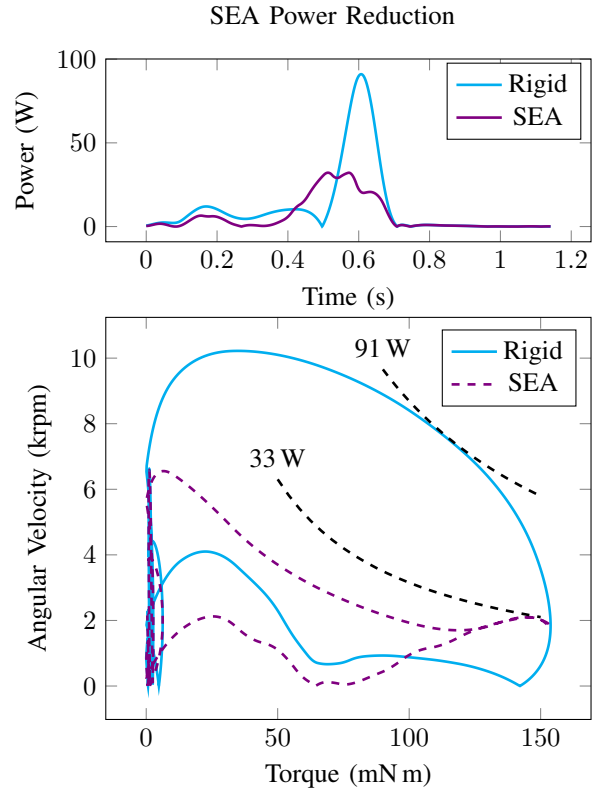


Fig. 1. SEA Power Reduction: Simulated power and velocity-torque trajectories for the motors of rigid linear and SEA PAFO actuators providing 30% of ankle torque for a single level-ground normal-speed (1.32 m/s) walking gait cycle for an 80 kg adult [18]. The peak power of the SEA motor is 64% less than that of the rigid actuator motor in this task.

270–380 W of power to the gait cycle in a process referred to as push off. Finally, during swing phase, the dorsiflexion muscles lift the toes so they do not drag on the ground.

Push off is the main source of power during level ground walking at normal speed [16] and motivates the powering of orthosis and prosthesis ankle joints. Lack of this power input reduces walking speed and increases the metabolic burden during locomotion [17].

B. Series Elastic Actuator

Hollander et al. [3] describe reduction of the motor's peak power requirement as the key benefit of an SEA for the design of PAFO. Fig. 1 illustrates this benefit. The upper plot shows the theoretical power consumption of two PAFO actuators providing torque equal to 30% of a healthy ankle's torque during one gait cycle. The rigid actuator's power consumption follows the solid curve, which peaks at 91 W. The SEA's power consumption, depicted by the dashed curve, has a much lower peak, 33 W. This 64% reduction of the peak power means that it is possible for an SEA to match the torque and speed performance of a rigid PAFO actuator while using a lower-power, lighter-weight motor, thus reducing the weight of the PAFO as a whole.

Hollander et. al. go on to derive an equation that shows the effect of an SEA's stiffness on its power consumption

during the walking cycle [3]:

$$P_m = \left| F\dot{x}_g + \frac{F\dot{F}}{K} \right|, \quad (1)$$

where P_m is the power consumed by the SEA motor, F is the SEA's output force, \dot{x}_g is the velocity of the SEA's output, and K is the SEA's stiffness. In this case, only K can be altered in order to reduce motor power since F , \dot{F} , and \dot{x}_g are determined from human gait trajectories such as those in [18].

Using Eq. 1 to calculate peak motor power, i.e. $\max(P_m)$, as a function of stiffness for three sets of walking trajectories yielded the plot in Fig. 2. The solid curve was generated using a human weight of 80 kg, and a walking speed of 1.68 m/s (equivalent to fast walking). On this curve, the minimum motor power occurs when SEA stiffness is 27.1 kN/m. However, the lower dashed curve, which was generated using the same human weight and a slower walking speed (1.32 m/s, normal walking), shows that peak power is minimal when stiffness is 19.9 kN/m. Therefore, the optimal stiffness for SEA motor peak power reduction varies with the speed of walking. The upper dashed curve was plotted using the first speed but with a different human weight. This curve has a minimum peak power value at yet another stiffness value, so optimal stiffness also varies with PAFO user weight.

Because the optimal stiffness for a PAFO SEA varies with gait parameters such as human weight and walking speed, it is desirable to have a PAFO SEA with a variable stiffness. Based on the experiment described in Sec. IV-C, the power required to change the stiffness of a DE elastic element is expected to be small, much less than the power savings the SEA architecture offers. Additionally, this variable stiffness could enable further reduction to the peak power requirements. If Eq. 1 is derived with K as time varying, the following equation results:

$$P_m = \left| F\dot{x}_g + \frac{F\dot{F}}{K} - \frac{\dot{K}F^2}{K^2} \right|. \quad (2)$$

The third term in Eq. 2 indicates that for a proper choice of SEA stiffness, K , and its rate of change, \dot{K} , the SEA motor peak power can be reduced even further than the reduction possible using a constant SEA stiffness.

C. Dielectric Elastomers as Variable Stiffness Elements

The previous section discussed the advantages of using a VSA for a PAFO. However, variable stiffness devices using conventional mechanical components tend to be complex and bulky. A DE is an alternative variable stiffness device that is mechanically simple and lightweight. A DE consists of an elastomer, a rubbery polymer, sandwiched between compliant electrodes as shown in Fig. 3. When the electrodes are electrically charged (oppositely), they attract each other and cause a compressive force on the sandwiched elastomer in the z-direction. Because of this compression, the elastomer expands in the x- and y-directions. This expansive effect can be harnessed for actuation.

Optimal SEA Stiffness Variation

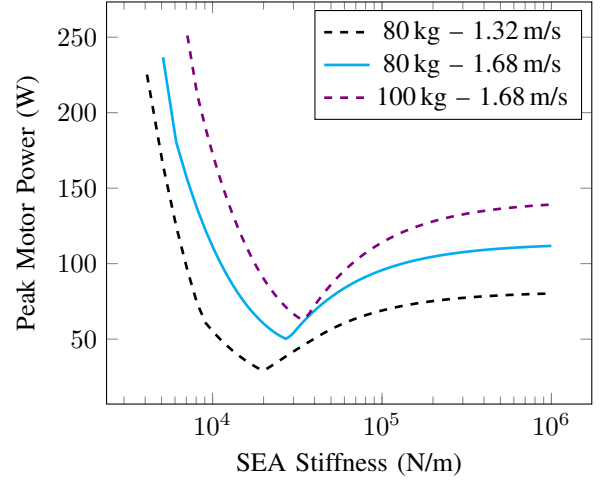


Fig. 2. Optimal SEA Stiffness Variation: The optimal stiffness for a PAFO SEA is the one that produces the lowest peak power during use. This optimal stiffness varies with gait parameters such as user weight and walking speed. Trajectories show peak motor power during a single gait cycle for a PAFO providing 30% ankle torque for three cases: an 80 kg user walking at normal speed (1.32 m/s), 80 kg user walking at fast speed (1.68 m/s) and a 100 kg user walking at fast speed (1.68 m/s).

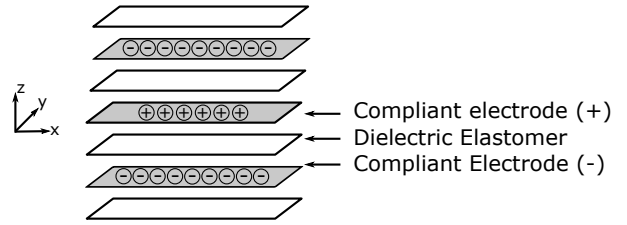


Fig. 3. Concept of Dielectric Elastomer: Charges applied to the compliant electrodes compress the dielectric elastomer layers causing them to expand in the x-y plane.

Charges on the electrodes also cause the stiffness of the DE to change. The motion of a DE charged with a constant voltage affects not only the mechanical energy stored in the elastomer, but also the electrical energy stored in the electrodes and the energy flowing from the electrical input. This electrical-mechanical energy conversion and electrical energy flow affect the mechanical stiffness of the DE. This process is described in more detail in [19].

In [19], Pelrine et al. derive an equation that relates the change of stiffness to the applied voltage for a planar DE with one end fixed, a load applied to its opposite end, and its width constrained:

$$k_{\text{eff}} = k_0 - bV^2. \quad (3)$$

Eq. 3 says that the effective DE stiffness in the actuation direction, k_{eff} , is reduced from the stiffness of the uncharged device, k_0 , by the square of the applied voltage, V , scaled by a constant (dependent on the elastomer's dimensions and electrical permittivity). Carpi et al. use this effect in their work [13]. A VSA with a DE as its elastic element could

take advantage of this effect so that the stiffness of the VSA could be modulated electrically.

III. ACTUATOR DESIGN

Our design, the Variable Series Elastic Actuator (VSEA), seeks to realize the benefits of a PAFO VSA using the theory described in Sec. II. In particular, using a DE as the variable stiffness element may enable this device to be lighter than comparable VSA.

The VSEA is a proof-of-concept linear actuator designed to be used in a test bed only. However, its performance and design constraints were derived from those necessary for an actual PAFO VSA as described in Sec. III-A. The design of the VSEA's elastic element is discussed in Sec. III-B. Finally, Sec. III-C gives a description of the actual design.

A. Design Requirements

The VSEA meets the force, speed, and travel requirements of a linear actuator driving a PAFO to provide 30% of the normal ankle torque of an 80 kg human during normal (1.32 m/s) and fast (1.68 m/s) walking. In this conceptual role, it would be positioned behind the wearer's calf with its motor end connected to the upper portion of the PAFO, and its output end connected to a 9 cm lever arm that actuates the wearer's ankle.

The force and speed output requirements for the device were derived from the sagittal plane motion of a human ankle. This simplification is justified given that the majority of the mechanical work performed during human walking is to create body-weight support and forward progression, both of which occur in the sagittal plane [16]. The ankle position and torque trajectories used for analysis came from data given by Winter [18]. Based on this data and the design assumptions in the previous paragraph, the goals for the maximum output force, speed, and travel of the linear transmission are 468 N, 256 mm/s, and 457 mm respectively.

A direct drive ball screw provides "gear reduction" in a compact, lightweight package and converts the rotary motion of the motor to linear motion that interfaces readily with the planar elastomer sheets. Because of these benefits, we selected a ball screw, which has a 2 mm lead, therefore the VSEA motor must have a maximum speed no less than 6,600 rpm and maximum torque no less than 154 mN m as can be seen from Fig. 1. The optimal values of stiffness for the VSEA elastic element are those given in Sec. II-B: 19.9 kN/m and 27.1 kN/m for normal and fast walking, respectively.

B. Elastic Element Design

There are many possible mechanical configurations for DE. Stack, bending beam, diaphragm, and tube are some of the common options [19]. The selection of a particular configuration has a direct impact on the maximum strain, required voltage, force output, power density, and fabrication complexity of the device. The VSEA was designed to use rectangular DE stacked on each other. In this design, planar elastomer sheets are stacked in layers with electrodes between

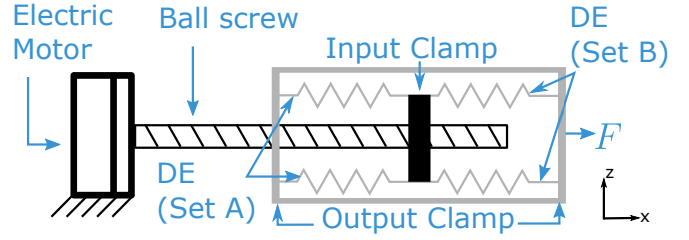


Fig. 4. Schematic Representation of VSEA Design: An electric motor drives a ball screw causing the input clamp to translate in the x -direction. The input clamp is elastically connected to the output clamp through two sets of DE (represented as springs). The load (F) is applied to the output clamp.

the elastomers as shown in Fig. 3. The stacks are clamped at their ends that are parallel to the y -axis, and then the motion of the VSEA clamps stretches and relaxes the sheets in the x -direction. The benefits of this configuration are comparatively simple manufacturing, a uncomplicated mathematical model, and ease of attachment to other mechanical components.

The VSEA design uses four stacks of DE configured to act as parallel springs that are intended to be solely in tension during operation. These stacks are depicted schematically as springs in Fig. 4. Those on the motor end of the actuator (set A) pull on the output clamp in opposition, antagonistically, to the force from the sheets on the output end of the actuator (set B). When set A extends, set B contracts, and vice-versa. This motion can be seen in the accompanying experimental video.

The first benefit of this configuration is that expansion of the DE in the x - y plane (mentioned in Sec. II-C) does not alter the equilibrium position of the output clamp. A second benefit is that because the antagonistic configuration is designed to keep the sheets in tension, the actuator can use their elastic effects whether it receives a tension or compression load.

The elastomer material was a proprietary urethane polymer. Its high dielectric constant (14) and dielectric breakdown strength (60 V/ μ m) enable it to undergo large stiffness reductions. Its failure strain and elastic modulus were well suited to the constraints of the project.

The dimensions of the sheets to be used in the stack DE configuration were constrained by several factors. First, the upper stiffness target constrained the overall geometry according to

$$k = \frac{nz w}{l} Y, \quad (4)$$

where k is the target stiffness value, n is the total number of sheets, z is the thickness of each sheet, w is the width of each sheet, and Y is the elastic modulus of the sheets. Second, to minimize sheet manufacturing and actuator assembly time, the number of sheets, n , needed to be minimized (sheet manufacturing can take days depending on the process). The manufacturing process limited the maximum length and width of the sheets to be either 10.2 cm or 9.2 cm. In order to minimize the actuation strain of the sheets, which is inversely proportional to their unstretched length, the sheet length was set to the larger of these values (10.2 cm). The width was then

TABLE I
DIELECTRIC ELASTOMER PARAMETERS

Parameter	Value	Units
Young's Modulus	2.5	MPa
Max. Strain	260	%
Dielectric Constant	14	–
Dielectric Strength	60	V/ μ m
Dimensions $l \times w \times z$ (nominal)		
Individual Sheet	114 \times 92.2 \times 0.2	mm
Active Area	63.5 \times 92.2 \times 0.2	mm

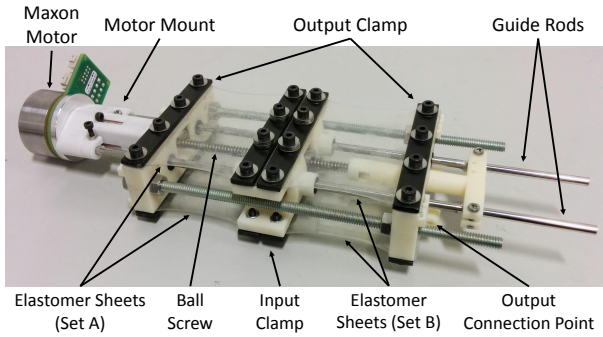


Fig. 5. Components of the Variable Stiffness Elastic Actuator: This novel device is a series elastic actuator. The motor mount is restrained with a pin joint. A Maxon motor drives a ball screw to cause linear translation of the input clamp. Elastomer sheets connect the input and output clamps forming an elastic connection between these elements. The load is connected to the output clamp at the output connection point.

chosen to be 9.2 cm in order to minimize n according to Eq. 4. Eq. 4 also suggests that z be maximized in order to reduce n , but increasing z also increases the voltage necessary to obtain the reduction between the upper and lower stiffness targets as can be derived from Eq. 3. A 200 μ m nominal sheet thickness put the voltage requirement near the upper limit of our high-voltage power supply. Table I summarizes the values selected for the VSEA elastic element.

C. Description of The Actuator

The overall layout of the actuator was driven by the desire to have a compact device utilizing 1) a direct drive ball screw, 2) planar elastomer sheets, and 3) an antagonistic spring configuration. Fig. 5 depicts the VSEA, which has a weight of 734 g and an overall length of 33 cm. The mechanical arrangement is as follows. The motor mount is fixed in place by a pin joint on the underside of the actuator. The motor mount supports two guide rods that serve as the backbone of the actuator. Screws hold a 70 W brushless DC motor (Maxon EC45 flat, P/N: 397172) to the motor mount, and a shaft coupler inside the motor mount connects the motor shaft to the end of the ball screw. The motor mount holds a bearing assembly that supports the ball screw's axial load. The ball nut travels along the ball screw as it rotates, and it connects to the input clamp through a pin joint. The ball

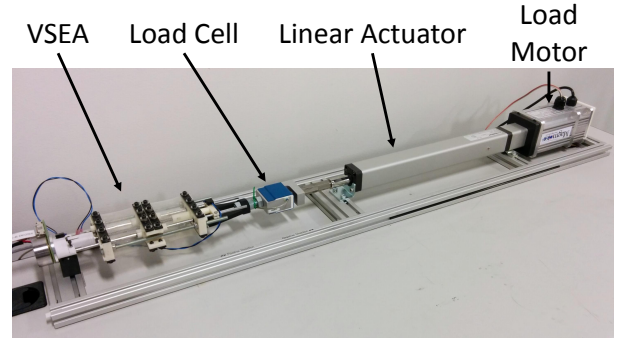


Fig. 6. Mechanical Test Bed for Testing Force and Position Output of VSEA: In this simple tensile tester, a load motor drives a linear actuator, which connects to the VSEA through a load cell. The load cell measures VSEA output force, and the positions of the VSEA's input and output clamps can be calculated from readings from encoders mounted on the VSEA and load motors.

screw has a lead of 2 mm; coupled with a 9 cm lever arm, it creates an approximate gear ratio of 272:1. Four black carbon fiber plates bolted to the input clamp clamp the inner ends of the elastomer sheets in place. The outer ends of the elastomer sheets are similarly clamped to the output clamp, and the two portions of the output clamp are connected with long bolts and nuts. This connection makes it possible to adjust the prestrain of the elastomer sheets. Some protrusions on the lower side of the output clamp allow the actuator to support a load through a pin connection. The accompanying video shows the motion of the actuator.

IV. EXPERIMENTS

A combination of two sets of trials, 1) force-displacement trials, and 2) a DE stiffness modulation trial, established the feasibility of using DE as a variable stiffness elastic element. The custom test bed for the force-displacement trials is described in Sec. IV-A. Sec. IV-B explains the force-displacement trials, which establish that elastomer films, the core structure of DE, are viable SEA elastic elements. The accompanying video illustrates these experiments. Subsequently, Sec. IV-C covers the DE stiffness modulation trial, that shows the stiffness of DE can be modulated enough to be useful for a PAFO VSA. Finally, Sec. IV-D discusses future direction for the project.

A. Description of Mechanical Test Bed

The mechanical test bed for the VSEA (depicted in Fig. 6) is essentially a simple tensile tester. The 300 W load motor (Magmotor BF34-200 brushless DC motor) sits at one end, and its output shaft is connected to a linear actuator. The VSEA is at the other end and connects to the linear actuator through a load cell. The linear actuator and the VSEA are connected to a T-slot frame.

The test bed features a load cell that measures the linear force output from the VSEA. Force measurements are recorded by a National Instruments myRIO 1900. Encoders attached to the VSEA motor and the load motor make it possible to determine the position of the VSEA's input and

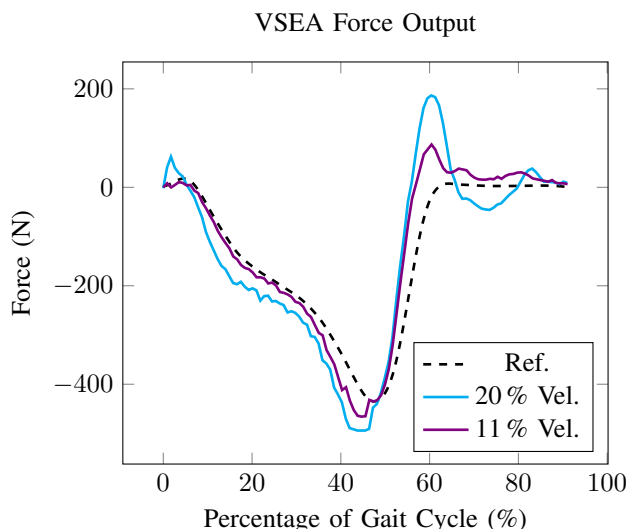


Fig. 7. VSEA Force Output: Dashed trajectories represent load cell measurements for VSEA open loop force control trials conducted at 20% and 11% of gait speed. Reference trajectory corresponds to the output force for a PAFO SEA providing 30% of normal ankle torque during normal-speed (1.32 m/s) level-ground walking for an 80 kg human. This data shows that the VSEA can provide enough force to significantly assist walking. Note that the VSEA force phase-leads and overshoots the reference trajectory, indicating significant viscoelastic behavior in the VSEA elastomer sheets.

output clamps respectively. From this information, the strain of the elastomer sheets can be calculated. The load motor and the VSEA motor were driven by separate Maxon EPOS2 70/10 motor drivers.

B. Force Testing Results

Three force-displacement tests were used to evaluate the performance of the VSEA. Two were open loop force control trials (Fig. 7), and one was a step displacement test (Fig. 9). In the two force control trials, closed loop position control drove the load motor along a position trajectory corresponding to the motion of an ankle during walking. At the same time, closed loop position control drove the VSEA motor along a position trajectory that was optimal for reducing the peak power of a PAFO SEA based on Eq. 1. Though the VSEA was designed to operate at speeds appropriate for normal walking, the motion during these two trials was scaled to slower speeds. The first trial was conducted at 20% of gait speed, so the trajectories took about 5 s to complete whereas a gait cycle takes about 1 s to complete. The second trial was conducted at 10.53% of gait speed. Full speed testing presents some difficulties for future work that will be discussed in Sec. IV-D.

The force trajectories obtained from the two trials are shown in Fig. 7. In this plot, the reference trajectory shows the desired force output of the VSEA over normalized time (% gait cycle). It corresponds to the output force for a PAFO SEA providing 30% of normal ankle torque during normal-speed (1.32 m/s) level-ground walking for an 80 kg human. The two other curves were obtained from load cell measurements during the trials. Though both of these curves approximate the

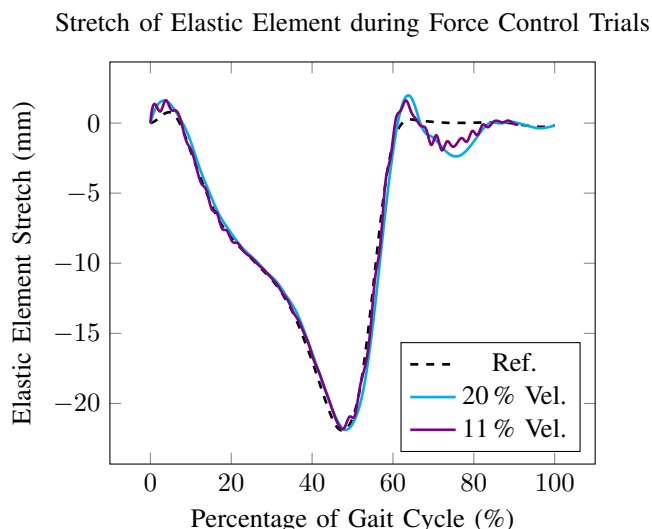


Fig. 8. Stretch of Elastic Element during Force Control Trials: This plot shows how the elastic element of the VSEA was stretched during the force control trials (same trials as for Fig. 7). The stretch followed the desired trajectory closely for most of the gait cycle indicating that position control was not a significant factor in the force control error seen in Fig. 7.

reference trajectory, they have some error. As Fig. 8 shows, position tracking control achieved the desired elongation of the elastomer based on the reference elastic model, especially in the time corresponding to 10–60% of the gait cycle; however, the force tracking error was significant even during this time period. The two solid curves of Fig. 7 are phase shifted ahead of the reference and overshoot its peaks. These effects are more pronounced in the curve corresponding to the faster trial indicating that the force output is velocity dependent. These characteristics can be explained by the presence of viscosity in the elastomer sheets, which cause the sheets’ stress (and thus their “spring force”) to be dependent not only on their strain but also their rate of strain.

The results of the step-displacement test, depicted in Fig. 9, confirm that the viscous nature of the elastomer sheets is not negligible and probably caused the force tracking discrepancies noted above. In this trial, the VSEA’s output clamp was held in place by the load motor, and the VSEA’s input motor quickly made a 10 mm displacement causing tension in the load cell. The dashed curve, obtained by multiplying the VSEA input clamp displacement by 19 kN/m, shows the theoretical force output from an elastic model of stress-strain behavior. This stiffness value was obtained by dividing the VSEA force at 4.9 s during the step-displacement trial (190.9 N) by the trial’s displacement of 10 mm and represents the theoretical elastic modulus of the elastomer sheets. The solid curve illustrates the actual force obtained from the trial. This curve greatly overshoots the reference curve and then gradually decays towards a steady-state value at approximately the level of the theoretical elastic steady state value. This behavior is characteristic of a viscoelastic material. The viscous effect is so strong that the peak force obtained from this trial, 319 N, is over 160% of the

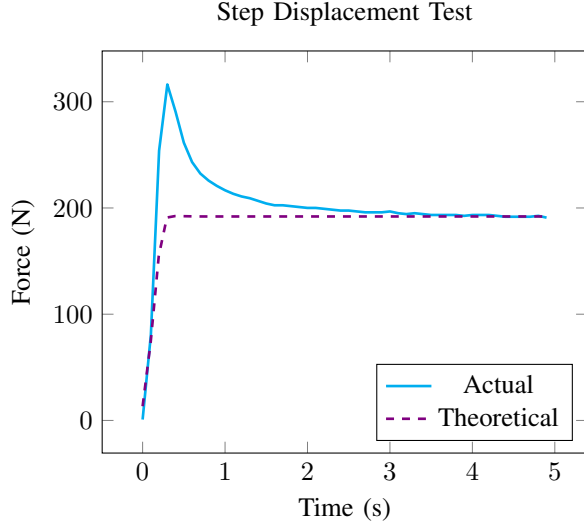


Fig. 9. Step Displacement Test: The VSEA elastomer sheets were rapidly stretched 10 mm. The theoretical force is the stretch of the sheets multiplied by 19 kN/m. This curve displays the theoretical elastic behavior of the elastomer films. The “actual” curve is the load cell measurements during the test. It rises faster than the elastic curve and dramatically overshoots it highlighting the viscoelastic behavior of the VSEA’s elastomer sheets.

theoretical elastic value (191 N). Clearly, the viscous nature of the elastomer sheets is not negligible, and it is almost certainly the primary cause of the force output discrepancies seen in Fig. 7.

Despite the issues caused by viscoelasticity, these trials clearly establish the viability of elastomer sheets as SEA elastic elements. The VSEA’s output force exceeded the peaks of the reference trajectory depicted in Fig. 7, so the VSEA’s force output is sufficient to assist with ankle torque for walking.

C. Variable Stiffness Testing

The preliminary VSEA assembly used for the experiments in this work did not have DE electrodes, so data from an off-board stiffness modulation trial is presented here. In this test, a urethane elastomer sheet with a nominal thickness of 100 μm was cut by a CO₂ laser into a 30 mm \times 100 mm rectangular shape. Nyogel 756G conductive carbon grease applied on both large faces of the sheet formed two flexible, rectangular (20 mm \times 50 mm) electrodes centered on those faces. The resulting DE was clamped into the tension assembly of a Lloyd LR5k Plus universal testing machine with a 100 N load cell. The DE was oriented with its long dimension in the loading direction. A high voltage power supply was attached to the electrodes. The DE was repeatedly stretched from 0–10 % strain at 50 mm/min and then relaxed. During each of these trials a constant voltage was applied to the DE. These voltages ranged from 0–5 kV in 1 kV increments. No more than a few microamps of current flowed across the DE during the trials. The tension and displacement data was used to calculate the stress and strain of the DE

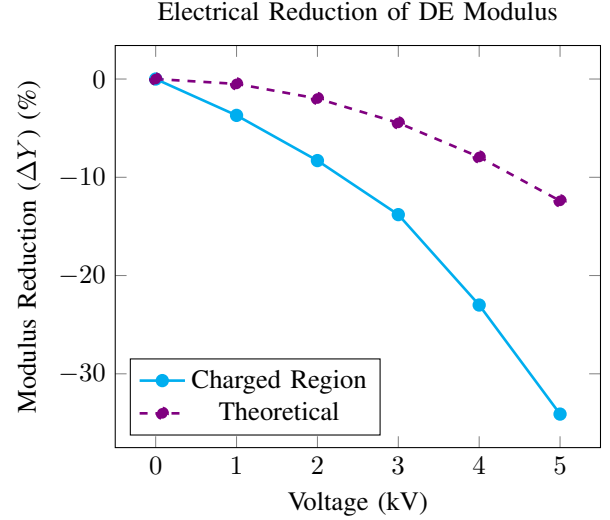


Fig. 10. Electrically Modulated Stiffness: Testing showed that the stiffness of DE reduces when greater voltage is applied to them. The DE tested displayed a stiffness variation wide enough to meaningfully improve VSEA performance. The theoretical values are based on Eq. 3.

and then its Young’s modulus, Y , according to

$$Y = \frac{\sigma_{\max}}{\varepsilon_{\max}},$$

where σ_{\max} is the maximum stress and ε_{\max} is the maximum strain of the sample obtained during each trial.

The reduction of the Young’s modulus of the charged area, Y_C , as a result of the charges applied to the DE is shown by the solid curve in Fig. 10. Assuming the electrodes have a negligible effect on the elastomer’s stiffness, the modulus reduction, ΔY , is:

$$\Delta Y = \frac{Y_C - Y_U}{Y_U} \times 100\%, \quad (5)$$

where Y_U is the Young’s modulus of the uncharged region of the elastomer. Modeling the charged and uncharged regions of the DE as parallel springs, Y_C is calculated starting with an equation for the effective modulus of the entire DE, Y_{eff} :

$$Y_{\text{eff}} = \frac{Y_U A_U + Y_C A_C}{A_U + A_C},$$

where A_C and A_U are the cross-sectional areas of the charged and uncharged regions of the DE respectively. Rearranging this equation yields:

$$Y_C = \frac{Y_{\text{eff}}(A_U + A_C) - Y_U A_U}{A_C}.$$

The modulus reduction for the charged region of the DE obtained from Eq. 5 is plotted in Fig. 10 as a solid curve. This data indicates that the DE modulus could be reduced more than 30 %.

The data from the variable stiffness test shows that the effective modulus of the DE decreases as the electric field applied to it increases, confirming the theory presented in Sec. II-C. This modulus reduction is directly related to stiffness reduction as Eq. 4 shows. Further, the stiffness of DE, using

the same urethane elastomer as that used in the VSEA, can be electrically modulated within a range wide enough to be useful for a PAFO VSA design. Sec. II-B indicated that a variation of walking speed could change optimal PAFO SEA stiffness from 27.1–19.9 kN/m, a 27 % reduction. The data in Fig. 10 shows that the stiffness of the VSEA could be reduced more than 30 %, which is a meaningful variation for this application.

D. Future Work

Based on the results of the VSEA force tests, it is clear that the viscous effects of the elastomers cannot be neglected, and an elastic model of their behavior is not appropriate. Future work will attempt to capture these effects with a viscoelastic stress-strain model. Then, this model can be used in future motion calculations for the device.

It is also desirable to conduct force testing at full gait speeds. A preliminary test at 50 % gait speed revealed issues with the test bed and the VSEA that affect testing capabilities and actuator safety, which should be corrected before further high performance tests. A redesign of the actuator may be necessary to ensure that it can handle higher force levels safely. Testing at full gait speed testing is planned to occur once these issues have been addressed.

The preliminary testing in this work confirmed the viability of DE as variable stiffness elements for a PAFO VSA. Future work will implement the stiffness modulation functionality on the VSEA itself. One hindrance of this goal is the practical difficulty of applying electrodes to the VSEA elastomer sheets. Future work will consider electrode options that can be manufactured in a repeatable and practical process such as the one detailed in [20].

Once the VSEA sheets are coated with electrodes, these electrodes can be used to measure the VSEA's force output. As described in [19], deformation of a DE changes the capacitance of its electrodes. This change can be easily measured and used to calculate the force output of the device. This process will be similar to how the force output of an SEA is obtained from Hooke's law and measurement of the SEA spring's displacement. However, the calculation for the VSEA will be more complex because the viscoelastic nature of the elastomer sheets make necessary their strain history to calculate the VSEA's output force.

V. CONCLUSION

PAFO design is in its infancy; there are none commercially available for home use at this time. Novel control theory makes it possible for PAFO to provide gait assistance in a natural fashion [21], but actuation technology holds the field back. Our work offers a new approach to actuation in this burgeoning field, specifically, enabling them to take advantage of the weight-saving characteristics of SEA and to tune the stiffness of an SEA without the weight and complexity penalties of current VSA. Our VSEA has demonstrated that it can produce a force output sufficient to provide meaningful gait assistance, and further development may be able to increase the force output further for only a mild penalty to the

VSEA's weight. The variable stiffness testing confirmed that it will be possible to tune the VSEA's stiffness to significantly reduce its peak power consumption as a PAFO actuator. This work has set the stage for future development of a pioneering approach to prosthetic and orthotic actuation.

REFERENCES

- [1] K. A. Shorter *et al.*, "Technologies for powered ankle-foot orthotic systems: Possibilities and challenges," *IEEE/ASME Trans. Mechatronics*, vol. 18, no. 1, pp. 337–347, 2013.
- [2] B. Vanderborght *et al.*, "Variable impedance actuators: A review," *Rob. Auton. Syst.*, vol. 61, no. 12, pp. 1601–1614, 2013.
- [3] K. W. Hollander *et al.*, "An efficient robotic tendon for gait assistance," *J. Biomech. Eng.*, vol. 128, no. 5, pp. 788–791, oct 2006.
- [4] R. Van Ham *et al.*, "Compliant actuator designs," *IEEE Robot. Autom. Mag.*, vol. 16, no. 3, pp. 81–94, 2009.
- [5] G. Grioli *et al.*, "Variable stiffness actuators: The user's point of view," *Int. J. Rob. Res.*, vol. 34, no. 6, pp. 727–743, 2015.
- [6] W. Friedl *et al.*, "FAS a flexible Antagonistic spring element for a high performance over actuated hand," *IEEE Int. Conf. Intell. Robot. Syst.*, pp. 1366–1372, 2011.
- [7] A. Jafari, N. G. Tsagarakis, and D. G. Caldwell, "A novel intrinsically energy efficient actuator with adjustable stiffness (AwAS)," *IEEE/ASME Trans. Mechatronics*, vol. 18, no. 1, pp. 355–365, 2013.
- [8] F. Petit *et al.*, "Bidirectional antagonistic variable stiffness actuation: Analysis, design & implementation," *Proc. - IEEE Int. Conf. Robot. Autom.*, pp. 4189–4196, 2010.
- [9] R. van Ham *et al.*, "Maccepa: the mechanically adjustable compliance and controllable equilibrium position actuator used in the controlled passive walking biped veronica," in *Proc. 2006 IEEE Int. Conf. Robot. Autom. 2006. ICRA 2006.*, no. May. IEEE, 2005, pp. 8–10.
- [10] M. Grebenstein *et al.*, "The DLR hand arm system," *Proc. - IEEE Int. Conf. Robot. Autom.*, pp. 3175–3182, 2011.
- [11] R. D. Kornbluh, R. E. Pelrine, and S. International, "Variable stiffness electroactive polymer systems," 2005, US Patent 6,882,086.
- [12] G. Berselli *et al.*, "Implementation of a Variable Stiffness Actuator Based on Dielectric Elastomers: A Feasibility Study," in *Vol. 1 Dev. Charact. Multifunct. Mater. Model. Simul. Control Adapt. Syst. Struct. Heal. Monit.* ASME, sep, p. 497.
- [13] F. Carpi *et al.*, "Enabling variable-stiffness hand rehabilitation orthoses with dielectric elastomer transducers," *Med. Eng. Phys.*, vol. 36, no. 2, pp. 205–211, feb 2014.
- [14] J. Shintake *et al.*, "Variable stiffness actuator for soft robotics using dielectric elastomer and low-melting-point alloy," *IEEE Int. Conf. Intell. Robot. Syst.*, vol. 2015-December, pp. 1097–1102, 2015.
- [15] L. Ren *et al.*, "A Phase-Dependent Hypothesis for Locomotor Functions of Human Foot Complex," *J. Bionic Eng.*, vol. 5, no. 3, pp. 175–180, 2008.
- [16] R. R. Neptune, S. A. Kautz, and F. E. Zajac, "Contributions of the individual ankle plantar flexors to support, forward progression and swing initiation during walking," *J. Biomech.*, vol. 34, no. 11, pp. 1387–1398, 2001.
- [17] S. Nadeau *et al.*, "Plantarflexor weakness as a limiting factor of gait speed in stroke subjects and the compensating role of hip flexors," *Clin. Biomech.*, vol. 14, no. 2, pp. 125–135, 1999.
- [18] D. Winter, *Biomechanics and motor control of human gait: normal, elderly and pathological*, 2nd ed. Waterloo: Waterloo Biomechanics, 1991.
- [19] F. Carpi *et al.*, *Dielectric Elastomers as Electromechanical Transducers: Fundamentals, Materials, Devices, Models and Applications of an Emerging Electroactive Polymer Technology*. Elsevier Science, 2008.
- [20] S. Rosset *et al.*, "Fabrication Process of Silicone-Based Dielectric Elastomer Actuators," *J. Vis. Exp.*, pp. 1–13, 2016.
- [21] G. Lv *et al.*, "Experimental Implementation of Underactuated Potential Energy Shaping on a Powered Ankle-Foot Orthosis," in *IEEE Int. Conf. Robot. Autom.*, 2016, pp. 4393–3500.